Transmembrane signal transduction in archaeal phototaxis: The sensory rhodopsin II-transducer complex studied by electron paramagnetic resonance spectroscopy

Klare, Johann P.; Bordignon, Enrica; Engelhard, Martin; Steinhoff, Heinz-Jürgen

European Journal of Cell Biology 90 (2011) 731–739

Contents lists available at ScienceDirect

European Journal of Cell Biology

journal homepage: www.elsevier.de/ejcb

Review

Transmembrane signal transduction in archaeal phototaxis: The sensory rhodopsin II-transducer complex studied by electron paramagnetic resonance spectroscopy

Johann P. Klare[a], Enrica Bordignon[a,1], Martin Engelhard[b], Heinz-Jürgen Steinhoff[a,*]

[a] Faculty of Physics, University of Osnabrück, Barbarastrasse 7, 49076 Osnabrück, Germany
[b] Max Planck Institute of Molecular Physiology, Otto-Hahn-Str. 11, D-44227 Dortmund, Germany

ARTICLE INFO

Keywords:
Phototaxis
Chemotaxis
HAMP domain
Transmembrane signalling
Signal transduction
Electron paramagnetic resonance spectroscopy
Site-directed spin labelling

ABSTRACT

Archaeal photoreceptors, together with their cognate transducer proteins, mediate phototaxis by regulating cell motility through two-component signal transduction pathways. This sensory pathway is closely related to the bacterial chemotactic system, which has been studied in detail during the past 40 years. Structural and functional studies applying site-directed spin labelling and electron paramagnetic resonance spectroscopy on the sensory rhodopsin II/transducer (*Np*SRII/*Np*HtrII) complex of *Natronomonas pharaonis* have yielded insights into the structure, the mechanisms of signal perception, the signal transduction across the membrane and provided information about the subsequent information transfer within the transducer protein towards the components of the intracellular signalling pathway. Here, we provide an overview about the findings of the last decade, which, combined with the wealth of data from research on the *Escherichia coli* chemotaxis system, served to understand the basic principles microorganisms use to adapt to their environment. We document the time course of a signal being perceived at the membrane, transferred across the membrane and, for the first time, how this signal modulates the dynamic properties of a HAMP domain, a ubiquitous signal transduction module found in various protein classes.

Introduction

The chemotaxis receptors of bacteria and archaea are members of a large superfamily of membrane proteins that modulate a signalling cascade known as the 'two component' phosphor transfer system (reviewed e.g. in (Stock et al., 2000)). The main components of this regulatory network are chemoreceptors, histidine and aspartate kinases, an SH3-like coupling protein and two proteins conveying adaptation to constant stimuli (Fig. 1A). Over the past 40 years considerable structural, kinetic and physiological information has been gathered, mostly by analysing the chemotaxis system of enteric eubacteria, in the first place *Escherichia coli* (for recent reviews see (Eisenbach, 2007; Hazelbauer et al., 2008; Suzuki et al., 2010)). The elucidation of colour-sensitive phototaxis in *Halobacterium salinarum* and in *Natronomonas pharaonis* has revealed a homologous organisation of the signal transduction chain in archaea (reviewed in (Engelhard et al., 2003; Hoff et al., 1997; Klare et al., 2007; Suzuki et al., 2010)). The receptors belong to the family of microbial rhodopsins, seven-helix transmembrane proteins carrying retinal as a chromophore. They are bound to cognate transducer molecules (halobacterial transducer of rhodopsin, Htr), whose cytoplasmic domains are highly homologous to the corresponding section of the chemotaxis receptors. In addition to two Htrs, at least 15 other methyl accepting proteins which resemble their eubacterial relatives have been identified in the *H. salinarum* genome (Alam et al., 1989; Alam and Hazelbauer, 1991; Ng et al., 2000). The congruence between the archaeal phototaxis and the bacterial chemotaxis system has been further established experimentally with a chimeric protein expressed in *E. coli*, comprising the photophobic receptor from *N. pharaonis* (*Np*SRII) and an N-terminal fragment of its cognate transducer (*Np*HtrII) fused to the cytoplasmic signalling and adaptation domains of *E. coli* chemotaxis receptors (Jung et al., 2001). Bacteria expressing these fusion proteins exhibited phototaxis (Jung et al., 2001) as well as light mediated autophosphorylation and transfer reactions (Trivedi and Spudich, 2003). The equivalence of the archaeal and eubacterial 'two component' signalling cascade combined with the knowledge about these systems provides the means to establish a model for investigating signal transfer across the membrane and to the cytoplasmic

* Corresponding author. Tel.: +49 541 969 2675; fax: +49 541 969 2656.
E-mail address: hsteinho@uni-osnabrueck.de (H.-J. Steinhoff).
[1] Present address: ETH Zürich, Laboratory of Physical Chemistry, Wolfgang-Pauli-Str. 10, CH-8093 Zürich, Switzerland.

0171-9335/$ – see front matter © 2011 Elsevier GmbH. All rights reserved.
doi:10.1016/j.ejcb.2011.04.013

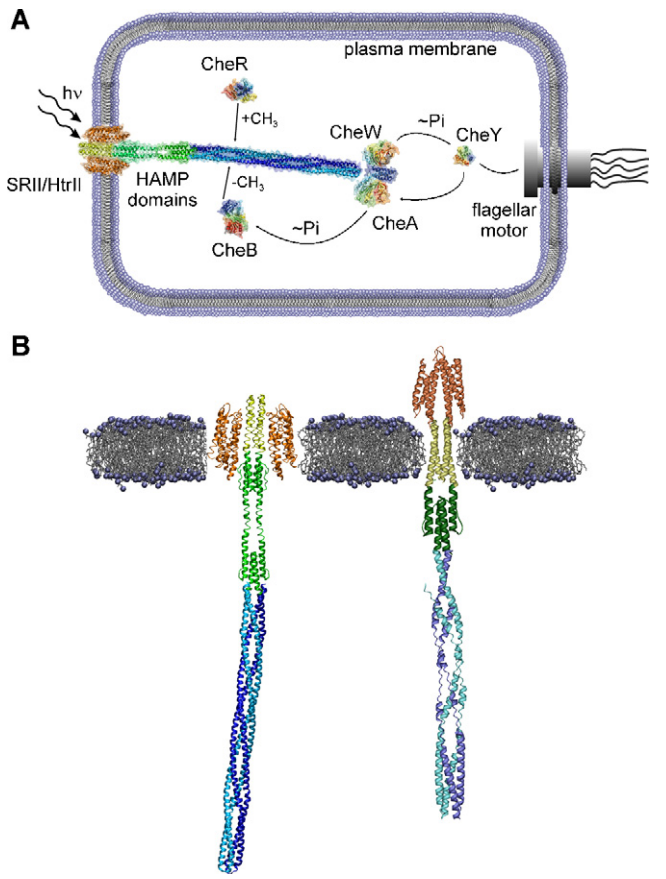

Fig. 1. (A) Two component phosphor transfer system. Light activation of the light receptor *Np*SRII triggers the activation of the phototransducer *Np*HtrII. The signal is transferred to the cytoplasmic end of the molecule, where it activates the homodimeric histidine kinase CheA bound together with CheW. The phosphate group is transferred from CheA to the response regulators/aspartate kinases CheY and CheB. CheY functions as a switch for the flagellar motor, whereas the methylesterase CheB together with the methyltransferase CheR mediates adaptation. (B) Models of the *Np*SRII/*Np*HtrII complex from *N. pharaonis* (left) and a eubacterial chemoreceptor (right) showing the architecture of the protein family. The photoreceptor *Np*SRII and the ligand binding domain in the chemoreceptor are shown in orange. The HAMP domain(s) – two in *Np*HtrII and one in the chemoreceptor – are shown in green. The cytoplasmic signalling/adaptation domains are depicted in blue/cyan.

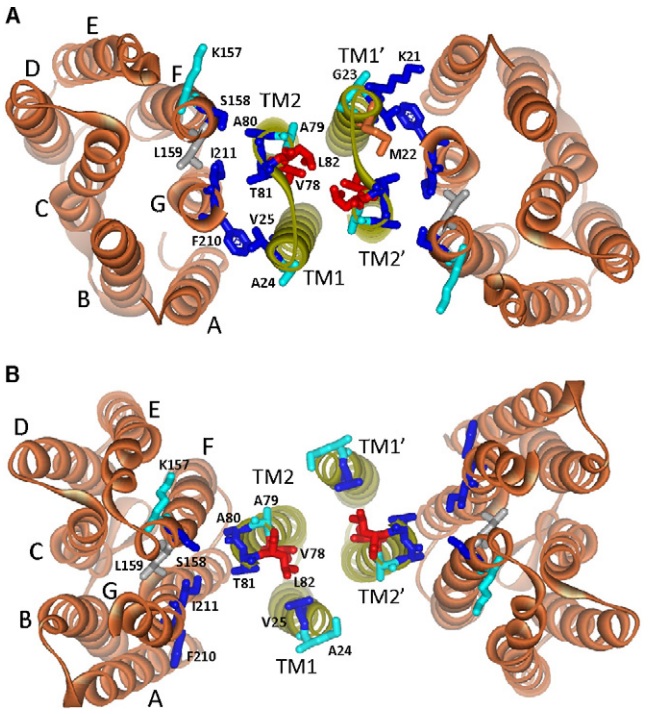

Fig. 2. (A) EPR based model of the transmembrane region of the *Np*SRII/*Np*HtrII complex viewed from the cytoplasmic side. Receptor helices are depicted in orange, transducer helices as yellow ribbons. Side chains mutated to Cys and subsequently labelled with MTSSL are shown in stick representation. The colour code represents the strength of the observed dipolar interaction (blue and red: strong; cyan and orange: weak). (B) Crystal structure of *Np*SRII/*Np*HtrII (pdb: 1H2S). Colour code is the same as in (A) (Klare et al., 2004b).

kinase on a molecular level. Here, we summarise the results of investigations on the structural and functional features of the archaeal *Np*SRII/*Np*HtrII complex using electron paramagnetic resonance (EPR) spectroscopy in combination with site-directed spin labelling (SDSL) (for recent reviews of this technique see (Bordignon and Steinhoff, 2007; Klare and Steinhoff, 2009, 2010)), which have been carried out during the past ten years in our laboratory.

Photo- and chemotactic systems

Light sensing in the haloarchaeon *H. salinarum* is mediated by two sensory rhodopsins which differentiate between light below and above 500 nm, respectively (Wolff et al., 1986). The first phototaxis receptor discovered was sensory rhodopsin I (SRI) which is expressed under low oxygen pressure and displays a dual function. In response to orange light, SRI (λ_{max} = 580 nm) directs the bacteria towards the light source. However, if in addition blue light is present, a two photon reaction triggers a photophobic response. SRI guides the bacteria into an environment optimal for the functioning of the two structurally closely related ion pumps bacteriorhodopsin (BR) and halorhodopsin (HR) which are concomitantly expressed when oxygen supply is ample. This latter condition is insufficient for cell growth, however the two ion pumps can supply the energy needs of the cell under such conditions (for recent reviews see (Engelhard et al., 2003; Spudich, 1998)). The second receptor, sensory rhodopsin II (SRII or phoborhodopsin), has its absorption maximum at 490 nm and enables the bacteria to avoid photooxidative stress under conditions of bright sun light in the presence of oxygen.

Sensory rhodopsins are seven helix (A–G) transmembrane proteins containing a retinal cofactor bound to a lysine residue on helix G *via* a protonated Schiff base (see Fig. 2B). On light excitation the retinal chromophore isomerises from the *all-trans* to a 13-*cis* configuration, triggering conformational changes which lead to the activation of the cognate transducer.

The general structure of the transducer molecules is quite similar to that of the chemoreceptors (Fig. 1B). A two-helix transmembrane domain is followed by a cytoplasmic domain, which contains the sub-domains for signal transfer to the histidine kinase CheA and for adaptation by reversible methylation of specific Glu residues. Between the N-terminal helix (TM1) and the following transmembrane helix (TM2) a periplasmic ligand binding domain is inserted in the chemoreceptors, which is also present in *Hs*HtrII (a serine receptor (Hou et al., 1998)) but not in HtrI or *Np*HtrII. The observation that *Hs*HtrII displays a dual functionality again strongly suggests a common mechanism of transmembrane signalling in photo- and chemotaxis. Nevertheless, a remarkable difference between the two classes of molecules is found at the interface between the transmembrane and the cytoplasmic domains. Although a so-called HAMP domain, a ubiquitous signal transduction module (Aravind and Ponting, 1999), succeeds TM2 in both classes of proteins, the chemoreceptors contain a single HAMP

domain, whereas all phototransducers exhibit two such domains connected by an α-helical linker.

In membranes, chemoreceptors as well as phototransducers form dimers which aggregate to higher order complexes (Bray et al., 1998; Maddock and Shapiro, 1993). Analogously, the phototransducers constitute a 2:2 complex with their cognate photoreceptors (Chen and Spudich, 2002; Wegener et al., 2001). The rod shaped cytoplasmic domains formed by the transducer dimers are arranged in an ~26 nm long four helical bundle. X-ray structures of the cytoplasmic domains have been resolved for the *E. coli* serine-chemoreceptor (Kim et al., 1999) and the *Thermotoga maritima* MCP_{1143} receptor (Park et al., 2006). These dimers or 2:2 complexes arrange in trimers, which in turn assemble with CheA and CheW to higher-order patches at the cell poles (recently reviewed in (Sourjik and Armitage, 2010)).

Structure of the membrane-embedded part of the *Np*SRII/*Np*HtrII complex

A topological model for the membrane-embedded portion of the complex was derived using data from our SDSL EPR experiments (Wegener et al., 2001). This methodology is a well suited technique for structural investigations, especially for membrane proteins (Bordignon and Steinhoff, 2007; Klare and Steinhoff, 2009). Nitroxide-scanning experiments provide sequence correlated data of the mobility of the replaced residue as well as their accessibilities for paramagnetic reagents. The latter allows differentiating between solvent exposed side chains, residues located in the hydrophobic region of a lipid bilayer and positions which are buried in the interior of the protein. Furthermore, evaluation of intra- and intermolecular spin–spin interaction provide distance constraints which allow the construction of topological models of single proteins as well as of protein complexes.

For modelling of the transmembrane portion of the complex, a transducer construct truncated C-terminally at position 157, $NpHtrII_{157}$, was used and the proteins were mutated and subsequently labelled with the nitroxide spin label MTSSL ((1-oxyl-2,2,5,5-tetramethylpyrroline-3-methyl)methanethiosulfonate) yielding the unnatural side chain R1, at the cytoplasmic side close to their putative interaction region (Fig. 2A). The experiments were carried out in detergent-solubilised and membrane-reconstituted samples. The reconstitution of the receptor together with its transducer in a 1:1 stoichiometry into polar lipids isolated from purple membranes resulted in immobilisation of the nitroxide side chains of the transducer compared to the solubilised samples. In addition, the spectra of the single mutants V78R1 and L82R1 were dipolar broadened. The inter-spin distances, obtained by fitting of simulated EPR spectra to the experimental data determined at 160 K, were determined to be less than 12 Å. These results were explained by two TM2 helices facing each other with residues V78 and L82 located at the interface of the helices. The distances between the TM1 helices seemed to be larger as only the spectrum of M22R1 displayed a weak spin–spin interaction. The observation of spin–spin interaction for V78R1 and L82R1 pointed towards a 2:2 stoichiometry of the complex reconstituted in membranes, in contrast to a 1:1 complex observed in detergent.

To determine the topology of the *Np*SRII/*Np*HtrII reconstituted complex, we determined inter-residue distances between TM1 or TM2 of $NpHtrII_{157}$ and helices F or G of *Np*SRII. Five residues of TM1 (21–25), two residues of TM2 (80 and 81), two positions at the cytoplasmic edge of helix F (157, 158) and at the corresponding locations of helix G (210, 211) were chosen for these experiments. The obtained inter-spin distances were used as constraints for the topological arrangement of the *Np*HtrII/*Np*SRII complex in the predicted model, shown in Fig. 2A. The results revealed a quaternary complex with two $NpHtr_{157}$ and *Np*SRII molecules each, forming a structure with an apparent two-fold symmetry (Fig. 2A). Since the structure of *Np*SRII was not known at the time of these investigations, a bacteriorhodopsin crystal structure was used as a template (Essen et al., 1998). The transducer helices were modelled as canonical α-helices.

Later, attempts to crystallise the membrane-embedded part of the complex were successful and the X-ray structure could be obtained (Gordeliy et al., 2002). Crystallisation of the receptor/transducer-complex was carried out using a further shortened transducer comprising residues 1-114 (Hippler-Mreyen et al., 2003). The crystals were grown using the lipidic cubic phase crystallisation method (Landau and Rosenbusch, 1996) and the structure was solved to 1.94 Å resolution. The asymmetric unit contains one dimer with a crystallographic two-fold rotation axis located in the middle of the four helical bundle formed by TM1, TM2, TM1′ and TM2′. Helices F and G of the receptor are in contact with the transducer-helices (Fig. 2B).

A direct comparison of the EPR-model with the crystal structure (see Fig. 2A and B) emphasises their consistency. In particular, the general topology of the cytoplasmic "layer" investigated in the EPR study is in very good agreement with the crystal data. Notably, most of the side-chain orientations within the complex of the SDSL EPR model also coincide with those of the crystal structure.

Receptor activation

The absorption of a photon by the sensory rhodopsins leads to isomerisation of the retinal chromophore from the *all-trans* to the 13-*cis* conformation, followed by thermal relaxations which finally lead back to the initial state. The intermediates have been denoted K, L, M, N, and O states, in analogy to the BR nomenclature. Important for the activation event, a spectrally silent irreversible reaction between two M-states ($M_1 \rightarrow M_2$) with a time constant of about 3 ms (Chizhov et al., 1998) has been deduced from a detailed analysis of the photocycle. In BR this transition is correlated with the accessibility switch, which changes the access to the Schiff base from the extracellular channel to the cytoplasmic channel, representing the key event for the vectorial proton transfer (Lanyi, 1998). The $M_1 \rightarrow M_2$ transition has also been observed by Fourier-transform infrared spectroscopy clearly demonstrating amide bond changes without alterations of the chromophore bands (Hein et al., 2003). *In vivo* experiments using *H. salinarum* (Yan et al., 1991) are in agreement with the assumption that these conformational changes are connected to formation of the photo-signalling state. Deactivation appears to require the decay of the O state.

To elucidate light induced conformational changes of the receptor as a possible key step in the signal transfer mechanism, we determined EPR difference spectra of photo-activated states and the initial state for *Np*SRII variants with spin labels bound to the cytoplasmic ends of helices B, C, F and G (Bordignon et al., 2007; Wegener et al., 2000, 2001). These spectra revealed considerable light-induced changes of the motional restrictions of almost all spin label side chains under investigation, indicating a general structural rearrangement of the cytoplasmic moiety of *Np*SRII. Apparently, a light induced transient mobilisation of the nitroxide side chains at positions 158, 159 and 211 was observed. Since the nitroxide side chains at helix G positions 212 and 213, which are oriented towards helices B and C, did not show any considerable mobility change upon light activation, a large movement of helix G is unlikely. We concluded that the required transient increase of the accessible space for the spin label side chains at positions 158, 159 and 211 had to result from a flab-like outward movement of the cytoplasmic part of helix F. This conclusion was further supported by the observation that in the presence of the transducer

the transient difference spectrum determined for side chain position 158 is inverted: the accessible space for the reorientational motion of the nitroxide was decreased by the outward movement of helix F towards TM2 of the transducer. We analysed the helix-tilt in more detail utilising inter spin distance measurements between spin labels located at the cytoplasmic end of helices B, C, F and G. The results show that the amplitude of the outward tilt of helix F at its cytoplasmic end adds up to about 0.4 nm (Bordignon et al., 2007). A similar motion of the corresponding helix in BR had been revealed by various techniques including cryo-electron microscopy (Subramaniam and Henderson, 2000), X-ray structural analysis (Luecke et al., 1999; Sass et al., 1997), and EPR (Rink et al., 2000; Steinhoff et al., 2000). It was concluded, that this tilt of the cytoplasmic portion of the receptor helix F, which occurs during the $M_1 \rightarrow M_2$ transition (see chapter "Time-resolved detection of conformational changes"), triggers the activation of the transducer.

Receptor–transducer signal transfer

The structure of the *Np*SRII/*Np*HtrII complex (Fig. 2) reveals the transmembrane interaction domains between receptor and transducer. The close contact between helices F and TM2, depicted in more detail in Fig. 3A, clearly suggests that an outward tilt of the cytoplasmic part of helix F will collide tangentially with TM2, thereby inducing a rotary motion of the latter helix as indicated by the arrows in Fig. 3B. This event was analysed by EPR (Klare et al., 2004a; Wegener et al., 2001) with specifically spin-labelled transducer and receptor Cys mutations positioned on helices F and G as well as on TM1 and TM2. In particular, two observations were central to establish a model for receptor-transducer signal transfer. The first observation concerned the mobility changes of S158R1 and L159R1 upon light excitation. Whereas S158R1, which faces TM2, experiences a transient immobilisation, the opposite is observed for L159R1, which is oriented towards the interior of *Np*SRII (see Fig. 2). The second observation was that the dipolar coupling between positions V78R1 and V78R1′ decreased upon light excitation whereas the coupling between L82R1 and L82R1′ remained unchanged. This result is in agreement with the assumption of a rotary motion of TM2. Further support of this mechanism is provided by cross-linking experiments on Cys transducer mutants. Several positions in TM2 exhibited light dependent modulations in the cross-linking efficiency (Yang and Spudich, 2001). However, it should be emphasised that from the EPR data a piston like movement cannot be excluded which would – together with a rotation of TM2 – result in a screw-type motion. Indeed, such a type of conformational change was later also observed in the crystal structure of the late M (M_2) intermediate of the complex (Moukhametzianov et al., 2006), confirming the model proposed from our EPR studies.

Structure of the *Np*HtrII HAMP domain(s)

HAMP modules are found in a wide variety of proteins (they are conserved in Histidine kinases, Adenylyl cyclases, Methyl-accepting chemotaxis proteins, and Phosphatases) connecting signal input with signal output. This diversity in the context of function and environment implies common principles of signal relay. For *Np*HtrII, an analysis of the primary sequence reveals the presence of two HAMP domains separated by a stretch of ~30 amino acids. The HAMP domains are characterised by the presence of two predicted amphipathic helices (AS-1 and AS-2), which exhibit a heptad repeat motif typical for α-helical coiled-coil structures, connected by an unstructured linker region. In the case of *Np*HtrII, the linker region connecting the two HAMP domains is, from its primary sequence, also predicted to be α-helical. Despite this secondary structure prediction, an initial structural analysis of the first *Np*HtrII HAMP domain, carried out by nitroxide scanning of the AS-1 region, of selected positions in the following connector and of the AS-2 region revealed the presence of a defined secondary structure only for the first half of AS-1, whereas the remaining portion appeared to be highly dynamic, resembling a molten globule-like structure at low salt concentrations (Bordignon et al., 2005).

A breakthrough for understanding the structure and function of HAMP domains was the solution NMR structure of the HAMP domain from *Archaeoglobus fulgidus* showing a homodimeric, four helical, parallel coiled coil with an unusual interhelical packing (Hulko et al., 2006) (Fig. 4A). These authors suggested a model for signal transduction, in which "the HAMP domain alternates between the observed conformation and a canonical coiled coil" *via* concerted helix rotations (Hulko et al., 2006). Investigations on the (single) HAMP domain in the bacterial chemotaxis receptor Tar (Swain and Falke, 2007) as well as the aerotaxis sensor Aer (Watts et al., 2008) from *E. coli*, mainly performed by cysteine scanning and crosslinking, have been found to be in agreement with the *A. fulgidus* NMR structure.

A more detailed SDSL EPR study on the first *Np*HtrII HAMP domain investigating the structural and dynamic features dependent on salt concentration (Fig. 4B) and temperature revealed that the HAMP domain is engaged in a "two-state" equilibrium between a highly dynamic (*d*HAMP) and a compact (*c*HAMP) conformation (Doebber et al., 2008) (Fig. 5). The structural properties of the *c*HAMP conformation as proven by mobility, accessibility, and intra-transducer-dimer distance data were found to be in agreement with the four helical bundle NMR model of the HAMP domain from *Archaeoglobus fulgidus*. Thus, as the structure obtained by NMR on an unusual archaeal membrane protein of unknown function seems to well represent the *c*HAMP conformation of the transducer from *N. pharaonis* as well as those of the *E. coli* Tar and Aer HAMP domains, the parallel four-helical bundle structure is likely to represent at least one of the possible conformations of HAMP domains in general. This assumption is further supported by a recent crystallographic study, which revealed the same general structural features for three concatenated HAMP domains from the *Pseudomonas aeruginosa* soluble receptor Aer2 (Airola et al., 2010). Numerous crosslinking studies on chemoreceptor proteins (refer to (Hazelbauer et al., 2008) and references therein) and successful attempts to exchange HAMP domains between different receptor types even from different organisms without impairing their function (Appleman and Stewart, 2003; Appleman et al., 2003; Kanchan et al., 2009; Linder and Schultz, 2010) are in line with this finding.

Time-resolved detection of conformational changes

A detailed picture of the conformational changes occurring during the life time of intermediate M and the succeeding part of the photocycle evolved from our time resolved EPR spectroscopy data, which were correlated with the optical absorbance changes. The absorbance changes due to the alteration of the protein–chromophore interactions are characteristic for the isomerisation state of the retinal, the protonation state of the Schiff base, and changes in the conformation of the protein. The kinetic analysis of the time resolved EPR signals derived from spin labelled *Np*SRII revealed a mobilisation of the spin label side chain 159R1 (Fig. 6A) during the $M_1 \rightarrow M_2$ transition as a consequence of the outward tilt of helix F. Helix F reversed back to its initial state during the decay of intermediate O (Klare et al., 2004a; Wegener et al., 2000) (Fig. 6B, green trace). The time course of the thereby induced TM2 rotation was monitored by the distance change between V78R1 and V78R1′ within the transducer dimer (Fig. 6, red trace). Helix F movement and TM2 rotation were found to occur simultaneously with the $M_1 \rightarrow M_2$ transition. On the other hand, the back reactions of receptor and transducer seem to be decoupled as TM2 returns back

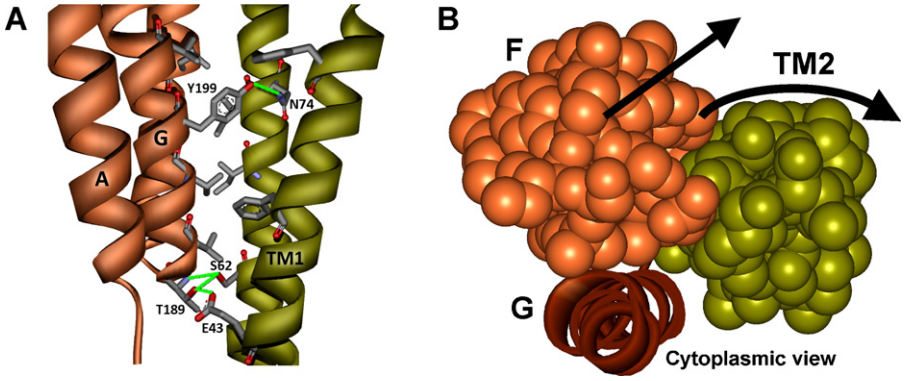

Fig. 3. (A) The interface between receptor (orange) and transducer (yellow) helices showing hydrogen bonds and van der Waals contacts. Residues involved in hydrogen bonding are labelled (Gordeliy et al., 2002). (B) Illustration of the light-induced conformational changes involving receptor helix F (orange) and transducer helix TM2 (yellow), shown in space-fill representation to stress the tight interaction between the two helices in the complex. The outward motion of the cytoplasmic portion of helix F and the subsequent rotary motion of TM2 are indicated by arrows (Klare et al., 2004a).

to its initial position with a delay of about 200 ms. Taking physiological data into account (Spudich et al., 1997), the signalling state is hence reached with the rotation of TM2. This active state is sustained even after the receptor has returned back to the initial state. A decoupling of the signalling state of the transducer from the state of the receptor molecule allows regulation of the transducer activity according to the cells physiological requirements.

Considering the two-state equilibrium between a compact and a dynamic HAMP conformation it is straightforward to ask, whether activation of the receptor/transducer complex by light could shift this equilibrium, thereby changing the signalling state of the transducer dimer. By applying time-resolved EPR spectroscopy we could indeed monitor changes in the dynamics of a spin label bound to position 100 in *Np*HtrII, which is located at the C-terminal end of AS-1 of the first HAMP domain (Fig. 6B, grey trace). Despite the low amplitude of the change of the EPR signal at this position (the amplitudes of the optical and EPR transient traces in Fig. 6 have been normalised for better comparison) it is obvious that the time course of the initial state recovery for M100R1 appears simultaneously with that of V78R1. (The formation of the activated state at position 100 could not be recorded due to the small signal-to-noise ratio). The amplitudes of the transient spectral changes are in line with a light induced transient immobilisation of the spin label at position 100 in accordance with a shift of the two-state equilibrium towards the compact HAMP conformation. Consequently, a compact HAMP structure would characterise the "kinase-on" state, which is in line

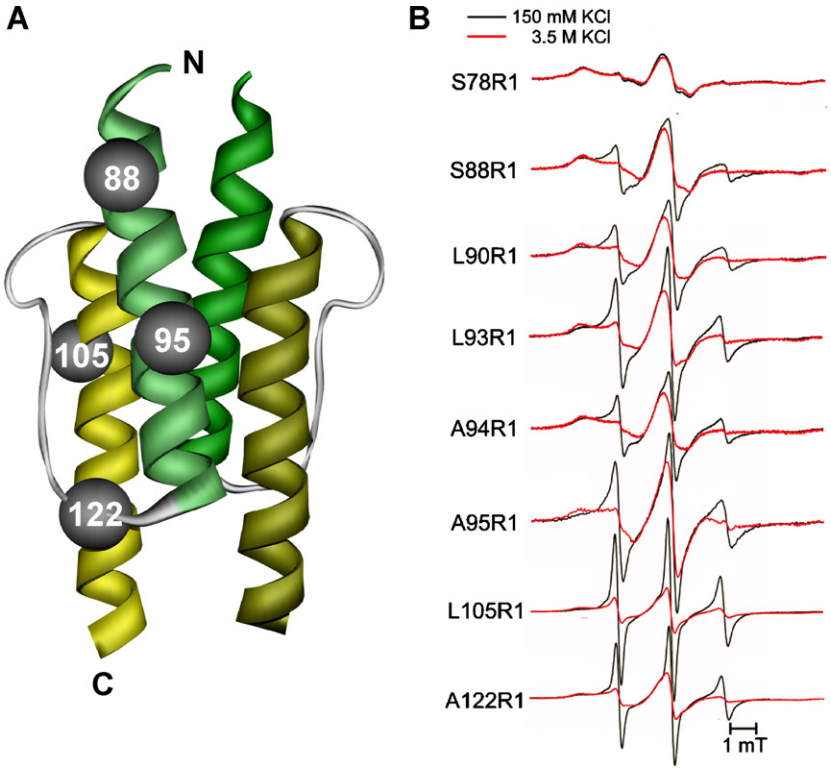

Fig. 4. (A) NMR structure of the *A. fulgidus* HAMP domain (pdb: 2ASW). Ribbon representation with the N-terminal helices (AS-1) depicted in green/dark green, the C-terminal helices (AS-2) in yellow/dark yellow and the connector regions in grey. Selected positions corresponding to the first *Np*HtrII HAMP domain are indicated as spheres at the Cα positions (Hulko et al., 2006). (B) Room temperature EPR spectra for spin labels bound to the indicated positions at the first *Np*HtrII HAMP domain. Spectra recorded at low salt concentration (150 mM KCl, black) and at nearly physiological salt concentrations (3.5 M KCl, red) reveal the presence of a salt dependent equilibrium between two HAMP conformations (Doebber et al., 2008).

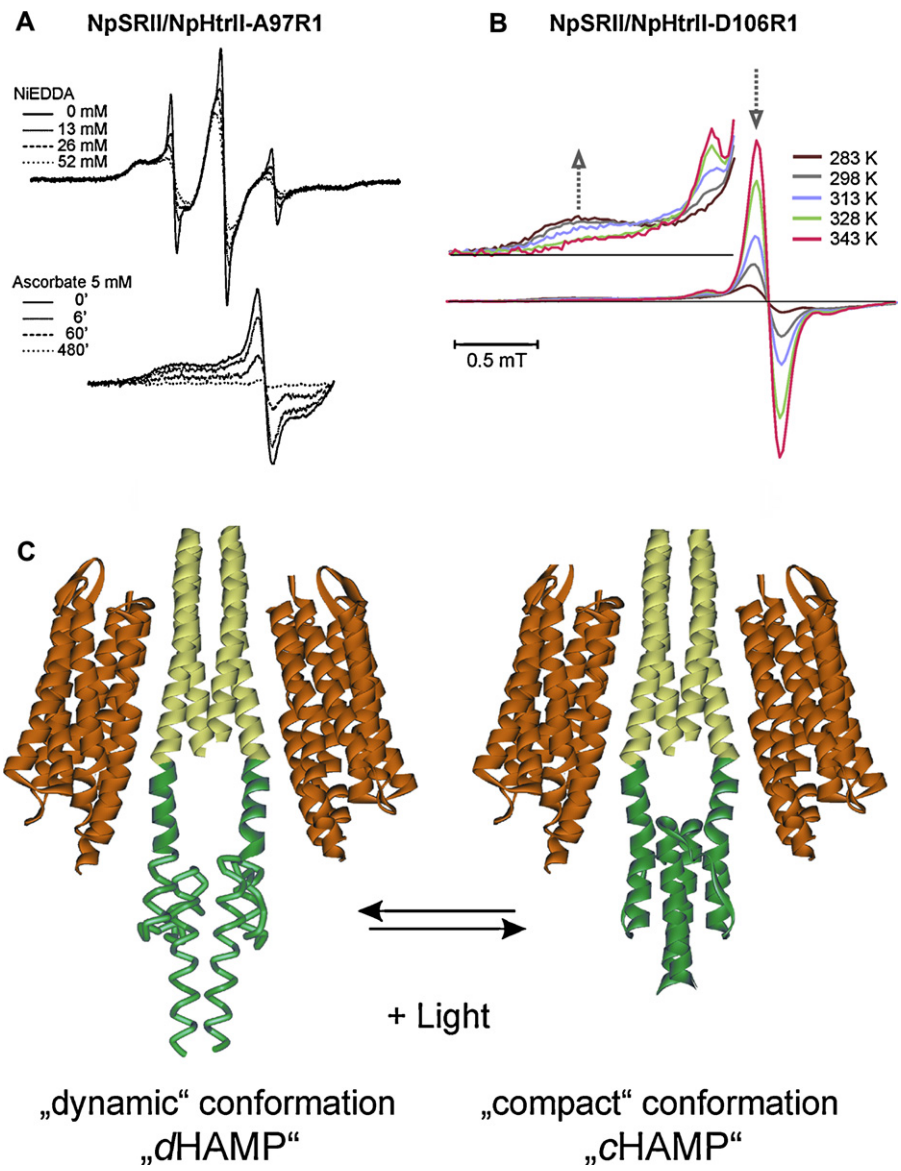

Fig. 5. Two HAMP conformations in equilibrium. (A) Effects of different NiEDDA concentrations (upper panel) and time evolution of ascorbate-induced spectral changes (bottom panel) on the two spectral components of *Np*SRII/*Np*HtrII$_{157}$-A97R1. The reversible quencher NiEDDA (upper panel) only affects the mobile component, indicating that only in this conformation is the spin label side chain accessible for the water soluble reagent. The irreversibly reducing agent ascorbate (bottom panel) affects both components in the same way, indicating a reversible equilibrium between the two conformational states. (B) Temperature-dependent spectral changes (low-field line) for *Np*SRII/*Np*HtrII$_{157}$-D106R1. Arrows indicate the direction of the spectral changes upon a decrease in temperature: the equilibrium is shifted towards the compact conformation. (C) Models of the dynamic and compact HAMP conformations. The compact conformation is modelled according to the NMR data of the HAMP domain of Af1503 from *Archaeoglobus fulgidus* (Hulko et al., 2006). EPR data indicate that the dynamic conformation resembles that of a molten globule state. Light activation of *Np*SRII shifts the equilibrium towards the compact state (Doebber et al., 2008).

with a recent cryo-electron microscopy study of TAR, where the authors observe a “compact” and an “extended” HAMP conformation in chemoreceptor trimers, the former corresponding to the “kinase-on” state (Khursigara et al., 2008).

Open questions

Three major questions remain, which are related to the function of the HAMP domain(s), the signal transfer from the cytoplasmic signalling domain of the phototransducer/chemoreceptor dimer to the histidine kinase CheA and, probably related to the second question, the impact of receptor clustering for the signalling process. We will discuss the first question in detail, as it is directly related to the results reviewed in this article, and just briefly address the other two questions.

Concerning the HAMP domains two unresolved but related issues are still obscure. First, how does signal transduction by HAMP domains take place? With the first NMR structure of a HAMP domain Hulko et al. proposed a model, in which the HAMP domain structure switches between the observed structure with an unusual side chain packing and a canonical coiled-coil structure by helix rotation – the so-called “gearbox”-model (Hulko et al., 2006). In contrast, based on the structure of three concatenated HAMP domains found to be in different “states”, Airola et al. (2010) propose the two conformations to be an in-register four-helix bundle and a distorted, more “open”, structure, respectively. Additional information comes from our EPR experiments on *Np*HtrII summarised in the preceding paragraphs, which revealed a switch between a compact and a dynamic HAMP conformation. Finally, a recent cryo-electron microscopy study on *E. coli* chemoreceptors showed that the HAMP domains within a receptor trimer were in

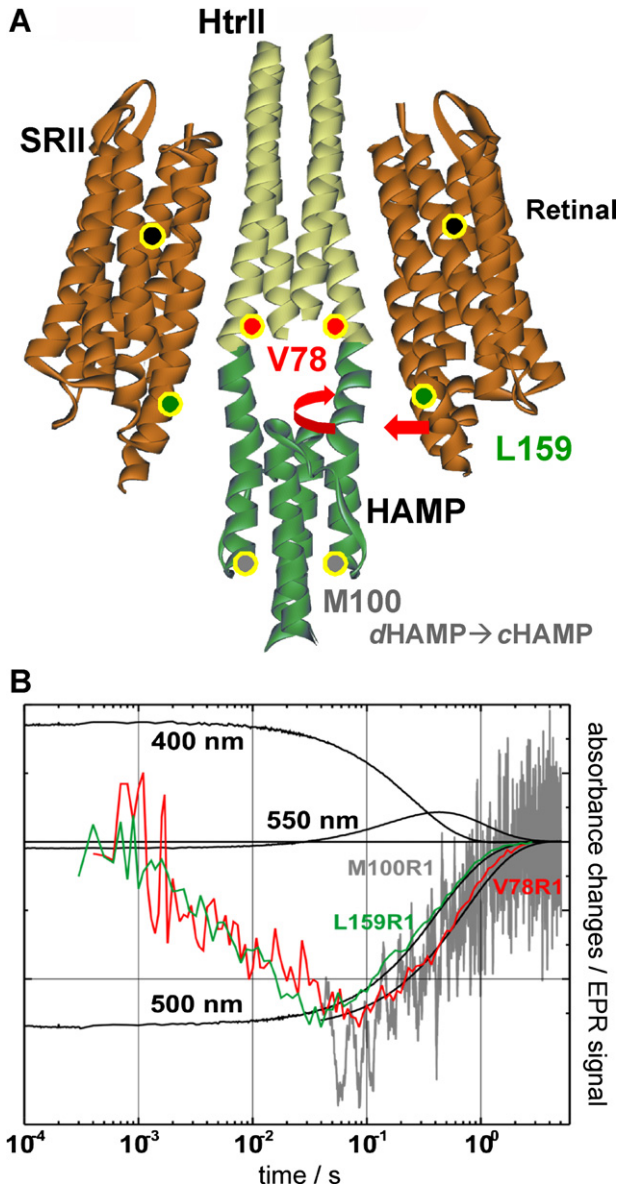

Fig. 6. Time-resolved detection of conformational changes. (A) Light excitation of the retinal chromophor in *Np*SRII leads to the outward motion of helix F (monitored at position 159) which induces a rotary motion of transducer helix TM2 (monitored at position 78). Helix rotation shifts the equilibrium between cHAMP and dHAMP towards the cHAMP conformation (monitored at position 100). (B) Optical (black) and transient EPR signals for L159R1 (green), V78R1 (red) and M100R1 (grey) (Klare et al., 2004a).

an equilibrium between a "compact" arrangement ("kinase-on") and an "extended" conformation ("kinase-off"), depending on ligand binding and methylation (Khursigara et al., 2008). With the exception of the "gearbox" model, which is based on theoretical considerations, all experimental results so far indicate that switching between a folded and a partially unfolded state is the basic mechanism of HAMP signalling. Consequently, the "output signal" could in turn modulate the dynamic properties of the following domains or switch between different structures by applying or releasing conformational strains.

Another still unresolved aspect of HAMP signalling is the question, why chemoreceptors contain a single HAMP domain, whereas the phototransducers have two HAMP domains connected by a helical linker region. The crystal structure of the three concatenated HAMP domains might give first indications for the physiological relevance of this systematic difference between the two protein classes. Based on the observation that three HAMP domains comprise both putative signalling states in alternating order, one could speculate that a second HAMP domain could simply invert the signal received from the first one. However, especially in the protein class of histidine kinases, up to 12 concatenated HAMP domains have been identified from the primary sequences. Thus, HAMP repeats might have another (additional?) function than just repeated signal inversion.

The second question, how signal transfer takes place from the signalling domain to the histidine kinase CheA, appears to be closely related to the first question. The output signals of the HAMP domains determine the conformation and/or dynamics of the cytoplasmic four helix bundle, for which structural details already exist from crystallographic studies (Kim et al., 1999; Park et al., 2006) (cf. Fig. 1B). Additional information about the possible arrangement of the ternary complex of the chemoreceptor signalling domain, CheA and CheW came from two extensive EPR studies (Bhatnagar et al., 2010; Park et al., 2006). Based on structural data and theoretical considerations, it has been speculated how the kinase activity could be modulated by different states of chemoreceptor dimers (Bhatnagar et al., 2010; Pollard et al., 2009) or subunit arrangements in trimer units (Suzuki et al., 2010). Nevertheless, a conclusive model for signal transfer has not been experimentally verified until now.

The third question, the role of receptor clustering in signalling, is closely related to the previous aspect. Numerous experimental studies and also theoretical considerations indicate that activation of one receptor molecule influences the signalling state also of neighbouring chemoreceptors, consequently leading to the modulation of the kinase activity of several CheA units. Furthermore, it is straightforward to envision that this fact also plays an important role for adaptation, as also chemoreceptors which have not encountered a direct stimulus themselves would be able to adapt to the environmental conditions. Therefore, the interaction between the proteins in these clusters is responsible for the remarkable properties of this signal transduction system: its high sensitivity (1% change in receptor occupancy induces a 50% change in the rotational bias of the flagellar motor), its high dynamic range, and its cooperativity (the Hill coefficients are >3 for Tar and >10 for Tsr (Sourjik and Berg, 2002, 2004)). The details of this interaction are still under discussion (Hazelbauer et al., 2008), but nevertheless, the mechanism of cooperative signalling can only be understood in detail, if it is known, how the signalling domain of a single receptor dimer is activated.

Conclusions and outlook

The research on the mechanisms underlying archaeal phototaxis and bacterial chemotaxis has been very fruitful during the past decade. The awareness that these two systems not only share the same concepts but are closely related, opened the opportunity to combine the wealth of data available to yield insight into the function of these systems on the molecular level. It has been demonstrated how external stimuli are perceived by receptor molecules or ligand binding domains and how these signals are transferred across the cell membrane. We begin to understand, how HAMP domains are involved in signal transduction and how nature uses these signal transduction modules to transfer information between protein domains – with impact not only for phototransducer/chemoreceptor molecules, but also for other substantial protein classes: histidine kinase, adenylate cyclases and phosphatases.

EPR spectroscopy therein contributed to the gain of knowledge about these systems. It is an excellent tool for structural investi-

gations, because it is the only methodology until today, which is able to provide structural information on the fully assembled signalling complexes. Moreover, information about the time course of signalling events within the photoreceptor/transducer complexes had been obtained with time resolved EPR spectroscopy.

Future research will address the function of these huge signalling complexes, which allow cells to sense and to adapt to their environment, and EPR spectroscopy will without doubt substantially contribute to resolve these questions.

Acknowledgements

This work was supported by the Deutsche Forschungsgemeinschaft (SFB 431, project P18).

References

Airola, M.V., Watts, K.J., Bilwes, A.M., Crane, B.R., 2010. Structure of concatenated HAMP domains provides a mechanism for signal transduction. Structure 18, 436–448.

Alam, M., Hazelbauer, G.L., 1991. Structural features of methyl-accepting taxis proteins conserved between archaebacteria and eubacteria revealed by antigenic cross-reaction. J. Bacteriol. 173, 5837–5842.

Alam, M., Lebert, M., Oesterhelt, D., Hazelbauer, G.L., 1989. Methyl-accepting taxis proteins in *Halobacterium halobium*. EMBO J. 8, 631–639.

Appleman, J.A., Chen, L.L., Stewart, V., 2003. Probing conservation of HAMP linker structure and signal transduction mechanism through analysis of hybrid sensor kinases. J. Bacteriol. 185, 4872–4882.

Appleman, J.A., Stewart, V., 2003. Mutational analysis of a conserved signal-transducing element, the HAMP linker of the *Escherichia coli* nitrate sensor NarX. J. Bacteriol. 185, 89–97.

Aravind, L., Ponting, C.P., 1999. The cytoplasmic helical linker domain of receptor histidine kinase and methyl-accepting proteins is common to many prokaryotic signalling proteins. FEMS Microbiol. Lett. 176, 111–116.

Bhatnagar, J., Borbat, P.P., Pollard, A.M., Bilwes, A.M., Freed, J.H., Crane, B.R., 2010. Structure of the ternary complex formed by a chemotaxis receptor signaling domain, the CheA histidine kinase, and the coupling protein CheW as determined by pulsed dipolar ESR spectroscopy. Biochemistry 49, 3824–3841.

Bordignon, E., Klare, J.P., Doebber, M.A., Wegener, A.A., Martell, S., Engelhard, M., Steinhoff, H.-J., 2005. Structural analysis of a HAMP domain, the linker region of the phototransducer in complex with sensory rhodopsin II. J. Biol. Chem. 280, 38767–38775.

Bordignon, E., Klare, J.P., Holterhues, J., Martell, S., Krasnaberski, A., Engelhard, M., Steinhoff, H.-J., 2007. Analysis of light-induced conformational changes of *Natronomonas pharaonis* sensory rhodopsin II by time resolved electron paramagnetic resonance spectroscopy. Photochem. Photobiol. 83, 263–272.

Bordignon, E., Steinhoff, H.-J., 2007. Membrane protein structure and dynamics studied by site-directed spin labelling ESR. In: Hemminga, M.A., Berliner, L.J. (Eds.), Biological Magnetic Resonance 27 – ESR Spectroscopy in Membrane Biophysics. Springer Science and Business Media, New York, pp. 129–164.

Bray, D., Levin, M.D., Morton-Firth, C.J., 1998. Receptor clustering as a cellular mechanism to control sensitivity. Nature 393, 85–88.

Chen, X., Spudich, J.L., 2002. Demonstration of 2,2 stoichiometry in the functional SRI-HtrI signaling complex in *Halobacterium* membranes by gene fusion analysis. Biochemistry 41, 3891–3896.

Chizhov, I., Schmies, G., Seidel, R.P., Sydor, J.R., Lüttenberg, B., Engelhard, M., 1998. The photophobic receptor from *Natronobacterium pharaonis*, temperature and pH dependencies of the photocycle of sensory rhodopsin II. Biophys. J. 75, 999–1009.

Doebber, M.A., Bordignon, E., Klare, J.P., Holterhues, J., Martell, S., Mennes, N., Li, L., Engelhard, M., Steinhoff, H.-J., 2008. Salt-driven equilibrium between two conformations in the HAMP domain from *Natronomonas pharaonis*, the language of signal transfer? J. Biol. Chem. 283, 28691–28701.

Eisenbach, M., 2007. A hitchhiker's guide through advances and conceptual changes in chemotaxis. J. Cell. Physiol. 213, 574–580.

Engelhard, M., Schmies, G., Wegener, A.A., 2003. Archaebacterial phototaxis. In: Batschauer, A. (Ed.), Photoreceptors and Light Signalling. Royal Society of Chemistry, Cambridge, pp. 1–39.

Essen, L.-O., Siegert, R., Lehmann, W.D., Oesterhelt, D., 1998. Lipid patches in membrane protein oligomers – crystal structure of the bacteriorhodopsin-lipid complex. Proc. Natl. Acad. Sci. U.S.A. 95, 11673–11678.

Gordeliy, V.I., Labahn, J., Moukhametzianov, R., Efremov, R., Granzin, J., Schlesinger, R., Büldt, G., Savopol, T., Scheidig, A.J., Klare, J.P., Engelhard, M., 2002. Molecular basis of transmembrane signalling by sensory rhodopsin II-transducer complex. Nature 419, 484–487.

Hazelbauer, G.L., Falke, J.J., Parkinson, J.S., 2008. Bacterial chemoreceptors, high-performance signaling in networked arrays. Trends Biochem. Sci. 33, 9–19.

Hein, M., Wegener, A.A., Engelhard, M., Siebert, F., 2003. Time-resolved FTIR studies of sensory rhodopsin II (NpSRII) from *Natronobacterium pharaonis*, implications for proton transport and receptor activation. Biophys. J. 84, 1208–1217.

Hippler-Mreyen, S., Klare, J.P., Wegener, A.A., Seidel, R.P., Herrmann, C., Schmies, G., Nagel, G., Bamberg, E., Engelhard, M., 2003. Probing the sensory rhodopsin II binding domain of its cognate transducer by calorimetry and electrophysiology. J. Mol. Biol. 330, 1203–1213.

Hoff, W.D., Jung, K.-H., Spudich, J.L., 1997. Molecular mechanism of photosignalling by archaeal sensory rhodopsins. Annu. Rev. Biophys. Biomol. Struct. 26, 223–258.

Hou, S., Brooun, A., Yu, H.S., Freitas, T., Alam, M., 1998. Sensory rhodopsin II transducer HtrII is also responsible for serine chemotaxis in the archaeon *Halobacterium salinarum*. J. Bacteriol. 180, 1600–1602.

Hulko, M., Berndt, F., Gruber, M., Linder, J.U., Truffault, V., Schultz, A., Martin, J., Schultz, J.E., Lupas, A.N., Coles, M., 2006. The HAMP domain structure implies helix rotation in transmembrane signaling. Cell 126, 929–940.

Jung, K.-H., Spudich, E.N., Trivedi, V.D., Spudich, J.L., 2001. An archaeal photosignal-transducing module mediates phototaxis in *Escherichia coli*. J. Bacteriol. 183, 6365–6371.

Kanchan, K., Linder, J.U., Winkler, K., Hantke, K., Schultz, A., Schultz, J.E., 2009. Transmembrane signaling in chimeras of the *Escherichia coli* aspartate and serine chemotaxis receptors and bacterial class III adenylyl cyclases. J. Biol. Chem. 285, 2090–2099.

Khursigara, C.M., Wu, X., Zhang, P., Lefman, J., Subramaniam, S., 2008. Role of HAMP domains in chemotaxis signaling by bacterial chemoreceptors. Proc. Natl. Acad. Sci. U.S.A. 105, 16555–16560.

Kim, K.K., Yokota, H., Kim, S.-H., 1999. Four-helical-bundle structure of the cytoplasmic domain of a serine chemotaxis receptor. Nature 400, 787–792.

Klare, J.P., Chizhov, I., Engelhard, M., 2007. Microbial rhodopsins, scaffolds for ion pumps, channels, and sensors. Results Problems Cell Differ. 45, 73–122.

Klare, J.P., Gordeliy, V.I., Labahn, J., Büldt, G., Steinhoff, H.-J., Engelhard, M., 2004a. The archaeal sensory rhodopsin II/transducer complex, a model for transmembrane signal transfer. FEBS Lett. 564, 219–224.

Klare, J.P., Bordignon, E., Engelhard, M., Steinhoff, H.-J., 2004b. Sensory rhodopsin II and bacteriorhodopsin, light activated helix F movement. Photochem. Photobiol. Sci. 3, 543–547.

Klare, J.P., Steinhoff, H.-J., 2009. Spin labeling EPR. Photosynthesis Res. 102, 377–390.

Klare, J.P., Steinhoff, H.-J., 2010. Site-directed spin labeling and pulse dipolar electron paramagnetic resonance. Encyclopedia Anal. Chem..

Landau, E.M., Rosenbusch, J.P., 1996. Lipidic cubic phases, a novel concept for the crystallization of membrane proteins. Proc. Natl. Acad. Sci. U.S.A. 93, 14532–14535.

Lanyi, J.K., 1998. The local-access mechanism of proton transport by bacteriorhodopsin. Biochim. Biophys. Acta 1365, 17–22.

Linder, J.U., Schultz, J.E., 2010. Transmembrane receptor chimeras to probe HAMP domain function. In: Melvin, I.S. (Ed.), Methods in Enzymology, Two-Component Signaling Systems, Part C. Academic Press, pp. 115–123.

Luecke, H., Schobert, B., Richter, H.-T., Cartailler, J.-P., Lanyi, J.K., 1999. Structural changes in bacteriorhodopsin during ion transport at 2 Angstrom resolution. Science 286, 255–260.

Maddock, J.R., Shapiro, L., 1993. Polar location of the chemoreceptor complex in the *Escherichia coli* cell. Science 259, 1717–1723.

Moukhametzianov, R.K., Efremov, R., Baeken, C., Göppner, A., Labahn, J., Engelhard, M., Büldt, G., Gordeliy, V.I., 2006. Development of the signal in sensory rhodopsin and its transfer to the cognate transducer. Nature 440, 115–119.

Ng, W.V., Kennedy, S.P., Mahairas, G.G., Berquist, B., Pan, M., Shukla, H.D., Lasky, S.R., Baliga, N.S., Thorsson, V., Sbrogna, J., Swartzell, S., Weir, D., Hall, J., Dahl, T.A., Welti, R., Goo, Y.A., Leithauser, B., Keller, K., Cruz, R., Danson, M.J., Hough, D.W., Maddocks, D.G., Jablonski, P.E., Krebs, M.P., Angevine, C.M., Dale, H., Isenbarger, T.A., Peck, R.F., Pohlschroder, M., Spudich, J.L., Jung, K.-H., Alam, M., Freitas, T., Hou, S., Daniels, C.J., Dennis, P.P., Omer, A.D., Ebhardt, H., Lowe, T.M., Liang, P., Riley, M., Hood, L., DasSarma, S., 2000. Genome sequence of *Halobacterium* species NRC-1. Proc. Natl. Acad. Sci. U.S.A. 97, 12176–12181.

Park, S.Y., Borbat, P.P., Gonzalez-Bonet, G., Bhatnagar, J., Pollard, A.M., Freed, J.H., Bilwes, A.M., Crane, B.R., 2006. Reconstruction of the chemotaxis receptor-kinase assembly. Nat. Struct. Mol. Biol. 13, 400–407.

Pollard, A.M., Bilwes, A.M., Crane, B.R., 2009. The structure of a soluble chemoreceptor suggests a mechanism for propagating conformational signals. Biochemistry 48, 1936–1944.

Rink, T., Pfeiffer, M., Oesterhelt, D., Gerwert, K., Steinhoff, H.-J., 2000. Unraveling photoexcited conformational changes of bacteriorhodopsin by time resolved electron paramagnetic resonance spectroscopy. Biophys. J. 78, 1519–1530.

Sass, H.J., Schachowa, I.W., Rapp, G., Koch, M.H.J., Oesterhelt, D., Dencher, N.A., Büldt, G., 1997. The tertiary structural changes in bacteriorhodopsin occur between M states – X-ray diffraction and Fourier transform infrared spectroscopy. EMBO J. 16, 1484–1491.

Sourjik, V., Armitage, J.P., 2010. Spatial organization in bacterial chemotaxis. EMBO J. 29, 2724–2733.

Sourjik, V., Berg, H.C., 2002. Receptor sensitivity in bacterial chemotaxis. Proc. Natl. Acad. Sci. U.S.A. 99, 123–127.

Sourjik, V., Berg, H.C., 2004. Functional interactions between receptors in bacterial chemotaxis. Nature 428, 437–441.

Spudich, E.N., Zhang, W., Alam, M., Spudich, J.L., 1997. Constitutive signaling by the phototaxis receptor sensory rhodopsin II from disruption of its protonated Schiff base - Asp73 interhelical salt bridge. Proc. Natl. Acad. Sci. U.S.A. 94, 4960–4965.

Spudich, J.L., 1998. Variations on a molecular switch – transport and sensory signalling by archaeal rhodopsins. Mol. Microbiol. 28, 1051–1058.

Steinhoff, H.-J., Savitsky, A., Wegener, C., Pfeiffer, M., Plato, M., Möbius, K., 2000. High-field EPR studies of the structure and conformational changes of site-directed spin labeled bacteriorhodopsin. Biochim. Biophys. Acta 1457, 253–262.

Stock, A.M., Robinson, V.L., Goudreau, P.N., 2000. Two-component signal transduction. Annu. Rev. Biochem. 69, 183–215.
Subramaniam, S., Henderson, R., 2000. Crystallographic analysis of protein conformational changes in the bacteriorhodopsin photocycle. Biochim. Biophys. Acta (BBA) – Bioenerg. 1460, 157–165.
Suzuki, D., Irieda, H., Homma, M., Kawagishi, I., Sudo, Y., 2010. Phototactic and chemotactic signal transduction by transmembrane receptors and transducers in microorganisms. Sensors 10, 4010–4039.
Swain, K.E., Falke, J.J., 2007. Structure of the conserved HAMP domain in an intact, membrane-bound chemoreceptor. A disulfide mapping study. Biochemistry 46, 13684–13695.
Trivedi, V.D., Spudich, J.L., 2003. Photostimulation of a sensory rhodopsin II/HtrII/Tsr fusion chimera activates CheA-autophosphorylation and CheY-phosphotransfer in vitro. Biochemistry 42, 13887–13892.
Watts, K.J., Johnson, M.S., Taylor, B.L., 2008. Structure–function relationships in the HAMP and proximal signaling domains of the aerotaxis receptor Aer. J. Bacteriol. 190, 2118–2127.
Wegener, A.A., Chizhov, I., Engelhard, M., Steinhoff, H.-J., 2000. Time-resolved detection of transient movement of Helix F in spin-labelled *Pharaonis* sensory rhodopsin II. J. Mol. Biol. 301, 881–891.
Wegener, A.A., Klare, J.P., Engelhard, M., Steinhoff, H.-J., 2001. Structural insights into the early steps of receptor–transducer signal transfer in archaeal phototaxis. EMBO J. 20, 5312–5319.
Wolff, E.K., Bogomolni, R.A., Hess, B., Stoeckenius, W., 1986. Color discrimination in halobacteria, spectroscopic characterisation of a second sensory receptor covering the blue-green region of the spectrum. Proc. Natl. Acad. Sci. U.S.A. 83, 7272–7276.
Yan, B., Takahashi, T., Johnson, R., Spudich, J.L., 1991. Identification of signaling states of a sensory receptor by modulation of lifetimes of stimulus-induced conformations. The case of sensory rhodopsin II. Biochemistry 30, 10686–10692.
Yang, C.-S., Spudich, J.L., 2001. Light-induced structural changes occur in the transmembrane helices of the *Natronobacterium pharaonis* HtrII transducer. Biochemistry 40, 14207–14214.